Investigating the reactivity of TiOx and BDD anodes for electro-oxidation of organic pollutants by experimental and modeling approaches

Jing Ma, Clément Trellu, Ekaterina Skolotneva, Nihal Oturan, Mehmet Oturan, Semyon Mareev

Investigationg the reactivity of TiO_x and BDD anodes for electro-oxidation of organic pollutants by experimental and modeling approaches

Jing Ma[1], Clement Trellu[1,*], Ekaterina Skolotneva[2], Nihal Oturan[1], Mehmet A. Oturan[1], Semyon Mareev[2,*]

1 Université Gustave Eiffel, Laboratoire Géomatériaux et Environnement EA 4508, 77454 Marne-la-Vallée, Cedex 2, France

2 Kuban State University, Physical Chemistry Department, 149 Stavropolskaya Str., 350040, Krasnodar, Russia

Manuscript submitted to Electrochimica Acta for consideration

Corresponding authors' email :

- Clément Trellu, clement.trellu@univ-eiffel.fr
- Semyon Mareev, mareev-semyon@bk.ru

Abstract

The reactivity of two non-active anodes (BDD and TiO_x) for the removal of organic pollutants from water was investigated and compared. A mathematical model for electro-oxidation of organic compounds was developed by considering (i) an analytical expression of the spatial distribution of $^{\bullet}OH$ concentration at non-active anodes, (ii) mass transport through the diffusion boundary layer and (iii) both direct electron transfer and $^{\bullet}OH$-mediated oxidation for degradation of organic pollutants. The model was calibrated from experimental data using, for example, terephthalic acid as $^{\bullet}OH$ probe molecule or ethanol as $^{\bullet}OH$ quencher during paracetamol degradation. Calculation of the fraction of current ascribed to the different possible reactions as well as a sensitivity analysis allowed for highlighting the key mechanisms and limiting phenomena. Degradation of organics occurs almost exclusively through $^{\bullet}OH$-mediated oxidation under mass transport limitation and for sufficiently high reaction rate constants. Improvement of degradation kinetics strongly depends on mass transport enhancement of organic compounds to the reaction zone at the electrode surface. Competition between the mother molecule and degradation by-products for reaction with $^{\bullet}OH$ did not significantly affect degradation kinetics under mass transport limitation. Direct electron transfer can potentially become important in presence of large amounts of $^{\bullet}OH$ scavengers or for organic compounds that react slowly with $^{\bullet}OH$ ($k<10^5$ m^3 mol^{-1} s^{-1}). Resuls also showed that the implementation of a suitable $^{\bullet}OH$ quenching experiment required the use of a concentration of ethanol of at least 100 mM for experiments performed at 5 mA cm^{-2} and with a concentration of target pollutant of 0.1 mM.

Keywords

Anodic oxidation, Hydroxyl radical, Modeling, Paracetamol, Terephthalic acid, Mass transport.

1. Introduction

Anodic oxidation (AO) is an electrochemical advanced oxidation process (EAOP) that is increasingly recognized as a promising next-generation technology for the treatment of contaminated effluents containing recalcitrant organic pollutants [1–5]. This process is based on the generation of a large amount of highly reactive hydroxyl radicals (•OH) from water discharge at the surface of suitable electrode materials [6–9]. The degradation of organic compounds through •OH-mediated oxidation is the key phenomenon for the non-selectivity of the process. Direct electron transfer (DET) at the anode surface can also participate in the degradation of organic pollutants. Thus, AO is able to achieve the complete degradation and mineralization of a large range of organic pollutants [10–20].

Anode materials have been classified in two main classes: active materials with low overpotential for oxygen evolution reaction (OER) and non-active materials with high overpotential for OER [4,7]. The latter ones are the most suitable for the accumulation of •OH at the anode surface. Among the variety of anode materials tested in the literature, the boron-doped diamond (BDD) appeared as the gold standard for application in the AO process [4,7–9,21]. However, this material is expensive and several researches are focused on the development of alternative non-active materials with lower production costs. Particularly, sub-stoichiometric titanium oxides (TiO_x) appeared as a promising material. Several recent papers have highlighted the capacity of this material to degrade and mineralize various organic pollutants [22–28].

The effectiveness of the AO process depends on (i) the reactivity of the anode material and (ii) mass transport conditions of organic compounds from the bulk to the reaction zone in the vicinity of the electrode surface. A crucial issue is related to the short lifetime of •OH. They are present only in a thin boundary layer (<1 μm) at the anode surface, which constitutes the reaction zone [29,30]. AO can be operated either under mass transport or current/kinetic control, depending on (i) convective-diffusive transport of pollutants from the solution to the reaction zone and (ii) oxidation rate in the reaction zone [4,31].

72 The development of suitable electrode materials requires a better understanding of the complex
73 phenomena occurring at the electrode/solution interface, including mass transport, •OH-mediated
74 oxidation and DET. Quantitative description of these phenomena and determination of the
75 optimal parameters for AO requires the combination of an experimental approach with an
76 adequate mathematical model. Several milestone contributions have been given in the literature.
77 First, Comninellis (1994) proposed a relation for the determination of the instantaneous current
78 efficiency depending on the nature of the electrode material (active or non-active), the
79 concentration of organic compounds and rate constants for oxidation of organic compounds and
80 O_2 evolution [6]. Then, Simond et al. (1997) have taken into account diffusion limitation [32].
81 Panizza et al. (2001) have also presented a macroscopic model describing the evolution of the
82 chemical oxygen demand (COD) according to the average mass transfer coefficient (k_m) and
83 current density [17]. This model supposes that oxidation of organic compounds is non-selective
84 and very fast. Scialdone et al. (2008, 2009) have further developed these approaches by taking
85 into consideration the oxidation pathway through DET [33] and the possibility of a limitation
86 from the oxidation rate at the anode [34]. Lan et al. (2018) have also worked on the consideration
87 of direct electro-oxidation at the anode surface [35]. Cañizares et al. (2004) proposed another
88 approach based on reactor-level description of the process [36]. Mascia et al. (2007) have
89 presented a 1-D model allowing the description of the concentration profile of organics
90 according to the distance from the electrode [37]. While Mascia et al. (2007) used lumped
91 parameters for the description of the concentration profile of •OH, Kapalka et al. (2009) have
92 then detailed the evolution of •OH at the surface of non-active anode in order to propose an
93 analytical expression for the spatial distribution of •OH concentration [29]. This approach
94 allowed for a more precise calculation of the thickness of the reaction zone. Several authors have
95 also proposed different ways to take into consideration other electrogenerated oxidants (active
96 chlorine, sulfate radicals), which might play an important role depending on both nature and
97 concentration of inorganic salts in the medium and reactivity of target compounds [35,38–40].

Finally, Misal et al. (2020) and Skolotneva et al. (2020) also developed models for electro-oxidation of organic compounds on porous electrodes in flow-through configuration [41,42].

Based on these previous works, a 1D model representing an AO mixed-tank reactor with either TiO_x or BDD plate anode operated under galvanostatic conditions was described in this study. The model took into consideration (i) convection/diffusion mass transport of organic compounds (ii) reaction of organics through DET and (iii) $^{\bullet}OH$-mediated oxidation of organics. This theoretical work was combined with a detailed experimental approach for the calibration of model parameters. Probe molecules and quenchers were used for determination and discussion of the role of $^{\bullet}OH$-mediated oxidation and DET. This works provides new insights on (i) the predominance of each mechanism in the degradation of organic pollutants, (ii) the identification of key parameters influencing the reactivity of BDD and TiO_x plate electrodes, (iii) competition phenomena between initial molecules and by-products and (iv) the assessment of the suitability of quenching experiments.

2. Material and methods

2.1 Chemicals

All chemicals used in this study were of reagent grade. Terephthalic acid (TA), paracetamol (PCT), sodium sulfate, sodium perchlorate and ethanol were purchased from Acros Organics, Sigma Aldrich, Honeywell Fluka, Alfa Aesar and Chimie-Plus Laboratoires, respectively. Solvents used for analysis were HPLC grade and purchased from Riedel-de-Haën. Solutions were prepared using ultrapure water (18.2 MΩ cm) from a Millipore Milli-Q system (Molsheim, France).

2.2 Electrode Materials

BDD plate (DIACHEM®) was obtained from CONDIAS (Germany), while Ti/TiO_x plate was supplied by Saint Gobain Research Provence. Dimensions of both plate electrodes were 8 x 4 cm. A carbon felt with the same dimensions was used as a counter electrode. Ti/TiOx plate was synthesized using plasma deposition on a Ti substrate, as detailed in a previous publication from our group [26]. A homogeneous coating was obtained on the surface of the Ti substrate as it can be observed from scanning electron microscopy (**Fig. SI-1**). The cross section view highlights that the thickness of the TiO_x coating was around 300 µm. XRD data are provided in **Fig. SI-2**. The TiO_x coating was made of a mixture of TiO_x phases, including Ti_4O_7 as the main phase. Preliminary tests showed that the electrode was stable in the range of operating conditions used in this study. Reproducible results were obtained during seven successive degradation kinetics. (**Fig. SI-3**).

2.3 Experimental oxidation of model compounds

Electrochemical oxidation of model compounds was carried out using an undivided electrochemical cell containing 300 mL of solution continuously mixed under magnetic agitation (750 rpm) (**Fig. SI-4**). The cell was operated under galvanostatic mode with an applied current density of 5 mA cm^{-2}. Sodium sulfate (0.05 M) was used as a supporting electrolyte. The anode and the cathode were placed in parallel with an inter-electrode gap of 2.5 cm. The geometric surface area of electrodes immersed in the solution was 23.6 cm^2.

A probe molecule was used in order to assess the reactivity of electrodes for •OH formation. TA (0.1 mM) was selected as the optimal compound, as suggested by Chaplin et al. [43] and other authors [44] in order to avoid false detection of •OH in electrolytic systems.

Another set of experiments was performed using PCT (0.1 mM) as a model compound. Quenching experiments were performed in order to assess the influence of different reaction mechanisms for the degradation of PCT [45–47]. Ethanol was added for quenching the influence

147 of both $^{\bullet}OH$ and $SO_4^{\bullet-}$. The molar ratio between ethanol and PCT was 1000:1. Tert-butyl alcohol
148 (TBA) was also used for quenching only the influence of $^{\bullet}OH$ in order to potentially highlight
149 the role of sulfate radicals.

150 For all the experiments, average values and standard deviations related to the evolution of the
151 concentration of organic compounds were obtained from triplicate experiments.

152

153 **2.4 Linear sweep voltammetry (LSV)**

154 A similar electrochemical cell was used for linear sweep voltammetry (LSV). LSV was
155 performed in 50 mM Na_2SO_4 at 10 mV s^{-1} using stainless steel as counter electrode and an
156 Ag/AgCl (3 M KCl) electrode as reference electrode. LSV curves were recorded from OCP
157 (open circuit potential) to 3.8 V. LSV data were corrected according to the uncompensated
158 resistance of the system.

159

160 **2.5 Mass transport**

161 The average mass transport coefficient (k_m) was obtained by using the limiting current density
162 method [22,48]. The limiting current (j_{lim}) for oxidation of 5 mM $Fe(CN)_6^{4-}$ was measured
163 through a CV scan in a similar electrochemical setup (using 100 mM $NaClO_4$ as supporting
164 electrolyte, stainless steel as counter electrode and an Ag/AgCl (3 M KCl) as reference electrode.
165 Excessive (20 mM) $Fe(CN)_6^{3-}$ was added in order to avoid any limitation from reactions at the
166 cathode. Mass transfer coefficient was calculated according to **Eq. 1**.

167 $$k_m = \frac{j_{lim}}{zFAC_b} \qquad \text{(Eq. 1)}$$

168 Where z is the number of electrons involved in anodic oxidation (z =1), F is Faraday's constant,
169 A is applied geometric surface area (m^2) and C_b is the concentration of $Fe(CN)_6^{4-}$ in bulk
170 solution (mol m^{-3}).

2.6 Quantification of organic compounds

Concentration of PCT was monitored by a Thermo Scientific UltiMate 3000 UHPLC system. An Hypersil Gold column (100×2.1 mm, 1.9 µm) was set in a thermostated compartment at 40 °C. The system was also equipped with an RS pump and a diode array detector (at 243 nm). The mobile phase was a mixture of methanol (15%) and phosphate buffer (5 mM Na_2HPO_4 and 7.5 mM H_3PO_4) (85%) with a flow rate of 0.1 mL/min.

The concentration of TA was measured by a Hitachi Elite LaChrom HPLC system equipped with a Purospher star RP-18e (5µm) column (set in a column oven at 40 °C), a UV detector L-2400 set at 254 nm and a pump L-2130. The mobile phase was a mixture of methanol (40%) and water containing 0.1% formic acid (60%) at a flow rate of 0.8 mL/min.

A TOC analyzer (Shimadzu TOC-L) was used for quantification of the mineralization yield of the treated solutions.

3. Calculations

Problem formulation and mathematical modeling is detailed in Supplementary Information (SI) file (See please **Text SI-1**). In short, the analytical expression for the spatial distribution of $^{\bullet}OH$ concentration was calculated according to Kapalka et al. (2009) [29], thus allowing to highlight the reaction zone at the electrode surface. Mass transport of organic compounds was considered to be limited by the diffusion boundary layer. Both $^{\bullet}OH$-mediated oxidation and DET were taken into consideration for degradation of organic compounds.

The mathematical problem was solved numerically by finite element method using the Comsol Multiphysics 5.6 commercial software package. Reliability of the calibration method was

assessed through the calculation of three statistical criterions used for process-oriented models, including root mean square error (RMSE), modelling efficiency (ME) and index of agreement (IoA) [49]. These values are given in **Table SI-1**. The values of ME and IoA were always higher than 0.97 and 0.993, respectively. A list of all model parameters is provided in **Table SI-2**. Parameters were obtained either from the literature or from experimental data, as indicated in **Table SI-2**. The methodology for calibration of unknown parameters is explained in the results and discussion section.

The calculations of fractions of current spent on the different possible reactions are detailed in Text SI-2 and SI-3.

4. Results and Discussion

4.1 Experimental determination of mass transport conditions

Mass transport conditions of dissolved compounds from the bulk to the electrode surface was characterized in the mixed-tank reactor by using the limiting current density technique in the ferro-ferricyanide system [48]. A current plateau was clearly observed using BDD electrode (**Fig. SI-6**), thus allowing for determination of the mass transport coefficient from **Eq. 1.** This coefficient was found to be k_m = 2.85 (± 0.31) x 10^{-5} m s^{-1}. By taking into account a diffusion coefficient of D = 7.26 x 10^{-10} m^2 s^{-1}, the thickness of the diffusion boundary layer (δ) was determined as 25.5 (± 2.3) µm using **Eq. 2**. These values are typical for plate electrodes implemented in mixed-tank reactors with high stirring rate [31].

$$\delta = \frac{D}{k_m} \qquad \text{(Eq. 2)}$$

From this value of k_m, it is possible to estimate the limiting current density according to **Eq. 3**, assuming a fast and non-selective reaction of organic compounds in the reaction zone [17]. For

the treatment of 0.1 M of TA or PCT, the limiting current density was calculated as 0.82 and 0.93 mA cm^{-2}, respectively. Thus, experiments performed in this study at j = 5 mA cm^{-2} were performed under strong mass transport limitation ($j > j_{lim}$).

$$j_{lim} = n\,F\,k_m C \qquad \textbf{(Eq. 3)}$$

where j_{lim} is the limiting current density (A m^{-2}), n is the number of electrons involved in mineralization of organic compounds (e.g., 30 for TA and 34 for PCT), F is the Faraday constant (96 485 C mol^{-1}) and C is the concentration of organic compounds in the solution (mol m^{-3}).

4.2 Oxygen evolution reaction

LSV (**Fig. 1**) allowed for characterization of OER. High potential for OER was observed for both materials by using the tangent method, i.e., 2.21 and 2.75 V *vs* Ag/AgCl for BDD and TiO_x, respectively. At these potentials, it is thermodynamically possible to form •OH from water oxidation since the thermodynamic potential of •OH is 2.13 V *vs* Ag/AgCl [29]. As already described in the literature, the complex mechanisms of OER at the surface of non-active anodes can be simplified in several successive reactions including first (i) water discharge and formation of •OH (**Eq. 4**) and (ii) reaction of •OH with each other for formation of H_2O_2 (waste reaction for •OH) (**Eq. 5**) [29,50].

$$H_2O \rightarrow {}^{\bullet}OH + H^+ + e^- \qquad \textbf{(Eq. 4)}$$

$$2\ {}^{\bullet}OH \rightarrow H_2O_2 \qquad \textbf{(Eq. 5)}$$

Weak adsorption of •OH at electrode surface (physisorption) is usually considered for this kind of electrode, therefore, •OH were considered as quasi-free. Reaction of •OH with the electrolyte and reaction with the electrode material (corrosion) were neglected. Thus, parameters related to

Eq. 4 were calibrated from LSV data (Fig. 1). The Butler-Volmer equation used to describe this reaction is given in SI (Eq. 10, SI) . The value of formal potential was obtained by the tangent method. Standard methodology was used for evaluation of kinetic parameters by plotting data in Tafel coordinate as described in the literature [51]. Values are reported in the recapitulative table in SI (**Table SI-2**). The fitting was low for $V_A < 2.2$ V *vs* Ag/AgCl (i.e. I < 50 mA) in the case of the BDD anode. As reported in the literature, it might be ascribed to the presence of surface redox couples or functional groups, which act as a barrier for OER on BDD anode [52]. However, the anodic oxidation process was then applied in the range of values of V_A and I for which the fitting was optimal.

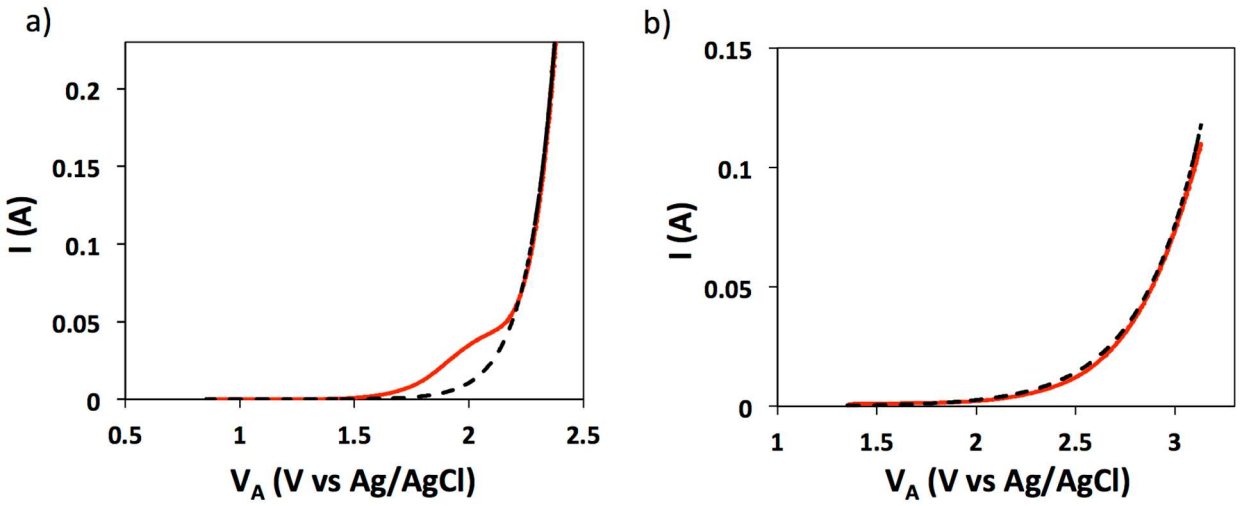

Figure 1 – Linear scanning voltammetry (10 mV s^{-1}) for characterization of oxygen evolution reaction on BDD (a) and TiO_x (b) anode in 50 mM Na_2SO_4. Red solid lines corresponds to experimental data while black doted line corresponds to the model.

It can be considered that further oxidation of H_2O_2 lead to the formation of O_2 (**Eqs. 6 – 7**) [29,50]. Thus, in the next sections of the manuscript, the fraction of current spent for O_2 evolution was calculated from the amount of $^{\bullet}OH$ reacting between each other (dimerization) (**Eq. 5**).

Formation of O_2 can also arise from oxidation of $^{\bullet}OH$ to atomic oxygen followed by formation of O_2 or O_3 (**Eqs. 8 – 10**). For sake of simplicity, these reactions were not taken into consideration in the model. The generation of $^{\bullet}OH$ was therefore considered as ideal. Thus, in the following sections, the calculated amount of $^{\bullet}OH$ available for reaction with target compounds must be considered as an upper limit.

$$H_2O_2 \rightarrow O_2 + 2\ H^+ + 2\ e^- \quad \text{(Eq. 6)}$$

$$H_2O_2 + 2\ ^{\bullet}OH \rightarrow O_2 + 2\ H_2O \quad \text{(Eq. 7)}$$

$$^{\bullet}OH \rightarrow O^{\bullet} + H^+ + e^- \quad \text{(Eq. 8)}$$

$$O^{\bullet} + O_2 \rightarrow O_3 \quad \text{(Eq. 9)}$$

$$2\ O^{\bullet} \rightarrow O_2 \quad \text{(Eq. 10)}$$

4.3 Hydroxyl radical mediated oxidation of a probe molecule (TA)

In a solution containing organic compounds, $^{\bullet}OH$-mediated oxidation of organic compounds represents an important pathway for disappearance of $^{\bullet}OH$. In fact, reaction rates between $^{\bullet}OH$ and organic compounds are usually in the same range ($k = 10^5 – 10^7$ m^3 mol^{-1} s^{-1}) [53] than reaction rate of $^{\bullet}OH$ between each other (**Eq. 5**) ($k = 5.5 \times 10^6$ m^3 mol^{-1} s^{-1}) [54]. There is a possible competition between the oxidation of organic compounds and this waste reaction (**Eq. 5**).

The capacity of BDD and Ti/TiO_x electrode for $^{\bullet}OH$-mediated oxidation of organic compounds was assessed using TA as probe molecule since it is strongly refractory to DET. It was observed that the degradation kinetic of TA followed a pseudo-first order degradation kinetic ($R^2 = 0.99$) with a rate constant of 0.009 min^{-1} and 0.017 min^{-1} for Ti/TiO_x and BDD anode, respectively. For modeling, the reaction rate of TA with $^{\bullet}OH$ was taken from literature ($k_{TA} = 3.3 \times 10^6$ m^3 mol^{-1} s^{-1}) [55]. Diffusion coefficient of TA was taken as equal to the one of PCT (the only one

available in the literature). The formation rate of •OH was calculated as an upper limit as described in sub-section 4.2. •OH-mediated oxidation was the only reaction pathway taken into consideration. Reaction of both TA and degradation by-products was taken into consideration. However, as described in sub-section 4.6 (sensitivity analysis), reaction of •OH with by-products do not affect degradation kinetics of the initial compound during these electro-oxidation experiments performed under conditions of mass transport limitation. Thus, the thickness of the diffusion boundary layer (δ) was the only key parameter calibrated for fitting the experimental data of TA degradation kinetics with BDD and TiO_x electrodes (**Fig. 2**). The obtained values of δ were 19 and 33 µm for BDD and TiO_x, respectively. It corresponds to mass transport coefficients of TA (k_m) of 3.42 x 10^{-5} and 1.97 x 10^{-5} m s^{-1} for BDD and TiO_x, respectively.

The calibrated value of δ was 25% lower for electro-oxidation of TA at BDD anode, compared to δ obtained in the ferro-ferricyanide system (i.e higher k_m during electro-oxidation of TA). As the generation of •OH available for reaction with organic compounds was calculated as an upper limit (sub-section 4.2), the calibration of more favorable mass transport conditions (lower δ) could not come from a compensation of an underestimation of the calculated amount of •OH. Therefore, lower value of δ could be ascribed to different operating conditions during electro-oxidation of TA, which modify the local hydrodynamic conditions at the anode surface. TA electro-oxidation occured in the potential region of water oxidation, while the ferro-ferricyanide system was operated at lower anodic potential. Therefore, formation of O_2 gas bubbles might strongly modify local hydrodynamic conditions at the electrode/solution interface. These results highlight that these local turbulences might enhance mass transport conditions in this configuration. Such local turbulences might also be influenced by surface roughness of the electrode.

The calibrated value of δ with TiO_x anode was 42% higher than the value obtained with BDD anode (i.e lower k_m during electro-oxidation of TA at TiO_x anode). It was even 29% higher than the value obtained in the ferro-ferricyanide system with BDD anode. It might be explained by

less favorable local mass transport conditions, related to physical properties of the electrode surface (e.g., hydrophobicity, local stagnant micro-volumes associated to different surface morphology / roughness). The calculated value of δ is a global parameter that averages heterogeneous mass transport conditions in the vicinity of the electrode surface. Another explanation might come from an overestimation of the calculated amount of •OH available for reaction with organic compounds. The higher calibrated value of δ (i.e. less favorable mass transport conditions) might be the result of the compensation of this overestimation. The TiO_x surface might further promote direct evolution of •OH to O_2 through **Eqs. 8-10**. Most probably, both phenomena (different mass transport conditions and different reactivity) might influence the lower TA degradation kinetic with TiO_x electrode. Suitable comparison of the reactivity of both electrodes would require to compare two electrodes with very similar physical properties (morphology / roughness, hydrophobicity).

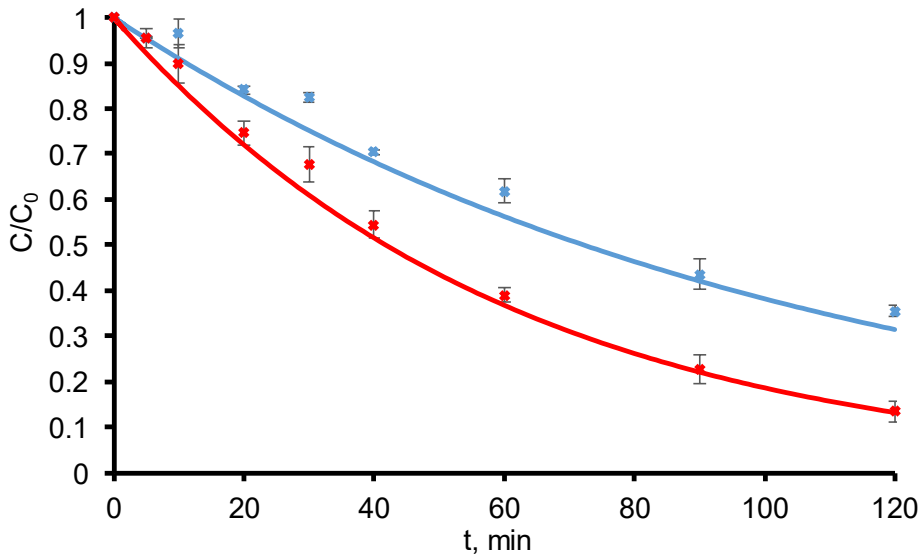

Figure 2 - Experimental (dots) *vs* model (lines) data for terephthalic acid degradation on BDD (red) and TiOx (blue) electrodes at 5 mA cm^{-2}. Error bars corresponds to triplicate experiments.

The calculated profile of concentration of •OH at electrode surface is presented in **Fig. 3B and SI-5B**. It followed a similar trend than previously reported by Kapalka et al. (2009) [29]. The calculated reaction layer thickness was about 0.8 µm with a maximum surface concentration of •OH around 20 µM. This concentration profile is usually affected by the concentration of organic compounds that can react with •OH. However, under the conditions of mass transport limitation of this study (sub-section 3.1), the concentration profile was not significantly affected as it can be seen from the absence of significant evolution during the treatment (i.e., decrease of concentration of organic compounds).

The evolution of the concentration of TA as a function of electrode distance can be divided into 3 main sections, including (i) the bulk solution where the concentration was considered as homogeneous ($x>19$ µm for BDD), (ii) the diffusion boundary layer where the concentration followed a linear decrease according to diffusion conditions ($0.8<x<19$ µm for BDD) and (iii) the reaction zone ($x<0.8$ µm) where organic compounds react with •OH (**Fig. 3A** for BDD and **Fig. SI-7A** for TiO_x). Calculations showed that TA concentration was 0 at the surface of both electrodes ($x = 0$), which is consistent with the operation of electro-oxidation under mass transport limitation.

Calculations allowed the estimation of the fraction of current spent on TA degradation from •OH-mediated oxidation (**Fig. 4**). It started from 0.67% and 0.39% for BDD and TiO_x, respectively. Then, these values continuously decreased during the treatment because of the decrease of the concentration of TA. The lower value obtained from TiO_x compared to BDD was ascribed from the model to the lower calibrated valued of k_m that reduces the amount of TA in the reaction zone where •OH are accumulated (comparison of **Fig. 3B** and **SI-5B**). However, as discussed above, it might also be ascribed to a lower concentration of •OH in the reaction zone since the formation of •OH is considered as ideal in the model.

The mineralization rate of by products (BP) is a complex phenomenon depending on the generation of various intermediates. For sake of simplicity, it was quantified by calibrating the

356 global reaction rate of degradation by-products (k_{BP}, **Eq. 14, SI**)) from experimental data of TOC
357 removal. Non-selective mineralization of by-products was considered [7]. The diffusion
358 coefficient of by-products was taken as equal to the one of TA. The total amount of •OH
359 consumed per molecule of by-product mineralized was calculated according to the equation
360 given in SI (Eq. 5, SI). A higher value of current was spent on mineralization of by-products as
361 the full mineralization of TA involves 30 electrons (instead of only 1 for initial degradation
362 step). However, the main part of current was spent on waste reactions (O_2 evolution) (**Fig. 4**). In
363 fact, electro-oxidation was operated under mass transport limitation, meaning that the amount of
364 •OH was in large excess compared to the amount of organic compounds. The lower the
365 concentration of organic compounds in the solution, the higher the level of waste reactions was.
366 The mineralization current efficiency (i.e., fraction of current used in reaction with organic
367 compounds) was initially at 11% and 1.8% and decreased to 3.8% and 1.4% after 2 hours of
368 treatment in the case of BDD and TiO_x, respectively. **Table 1** provides a comparison of the
369 efficiency (in terms of degradation kinetic and mineralization rate) achieved in this study with
370 results previously reported in the literature. It appears that these results were in the same range
371 than data reported in the literature for configurations operated under mass transport limitation.
372 However, it is difficult to compare rigorously such data since several operating parameters
373 influence the effectiveness of the process (pollutant concentration, current density, ratio between
374 electrode surface (S) and reactor volume (V)). For example, the influence of the S/V ratio is
375 further detailed in section 4.9 using a sensitivity analysis of the model.

376

377 **Table 1** – Comparison of the effectiveness of the anodic oxidation process in undivided mixed-
378 tank reactor. The mineralization current efficiency corresponds to the indicated TOC removal.

Anode	Pollutant [C] - mM	Current mA cm^{-2}	$S_{electrode}/V_{reactor}$ m^{-1}	TOC removal %	MCE[2] %	k_{app}[3] min^{-1}	Ref
Ti/TiO_x	Amoxicillin 0.1	5	10.4	40	5	0.03	[26]

BDD	Amoxicillin 0.1	5	10.4	80	10	0.05	[26]
BDD	p-ASA[1] 0.1	4.2	10.4	55	3.7	0.07	[56]
PbO_2	p-ASA[1] 0.1	4.2	10.4	55	4.2	0.05	[56]
Ti/TiO_x	p-ASA[1] 0.1	4.2	10.4	50	3.5	0.05	[56]
Pt	p-ASA[1] 0.1	4.2	10.4	37	2	0.02	[56]
BDD	orange G 0.52	33	3	50	4.5	0.01	[57]
BDD	orange G 0.52	150	3	80	13	0.02	[57]
BDD	paracetamol 0.52	100	3	30	4.7	-	[58]
BDD	paracetamol 6.3	100	3	15	28	-	[58]
BDD	TA 0.1	5	7.8	65	3.8	0.02	This study
Ti/TiO_x	TA 0.1	5	7.8	21	1.4	0.01	This study

[1] p-aminosalcilyc acid ; [2] mineralization current efficiency ; [3] pseudo-first order kinetic rate constant

It is interesting to notice that the difference of effectiveness of BDD and TiO_x was higher for mineralization of TA than for •OH-mediated degradation of TA. For example, TA degradation yield after 1 h of treatment was 60 and 37% for BDD and TiO_x, respectively, while TOC removal after 2 h of treatment was (65 ± 3)% and (21 ± 5)% for BDD and TiO_x, respectively. These results might be explained by (i) a better electrokinetic behavior of BDD for oxidation by DET of by-products reacting slowly with •OH (e.g. carboxylic acids) and/or (ii) a less favourable electrokinetic behavior of TiO_x for accumulation of •OH at its surface (e.g. further evolution of •OH through **Eqs. 8-10**)

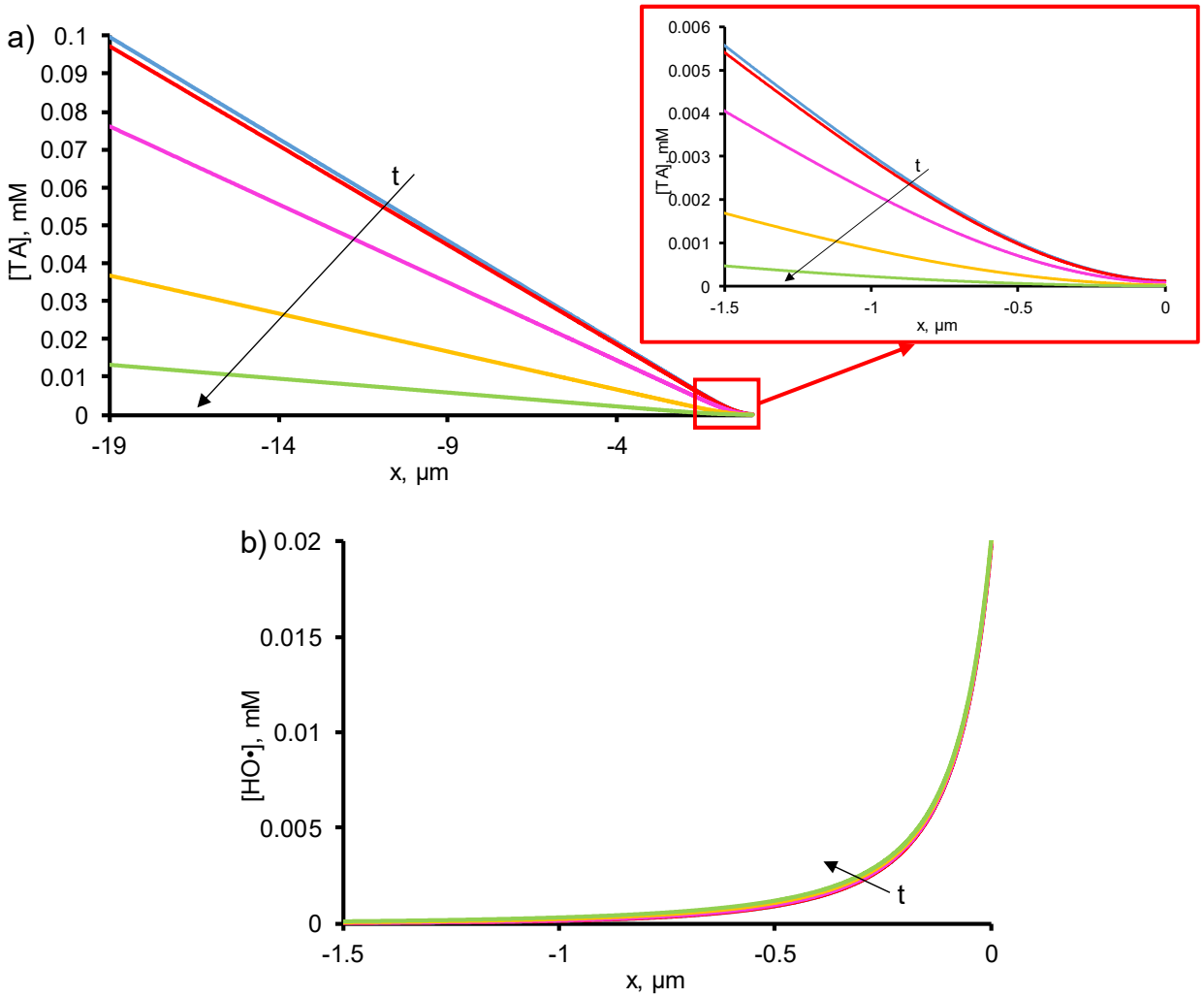

Figure 3 - Concentration profiles of terephthalic acid (TA) (a) and •OH (b) on BDD electrode during TA oxidation at t = 10 (blue), 100 (red), 1000 (pink), 3600 (yellow), 7200 (green) s.

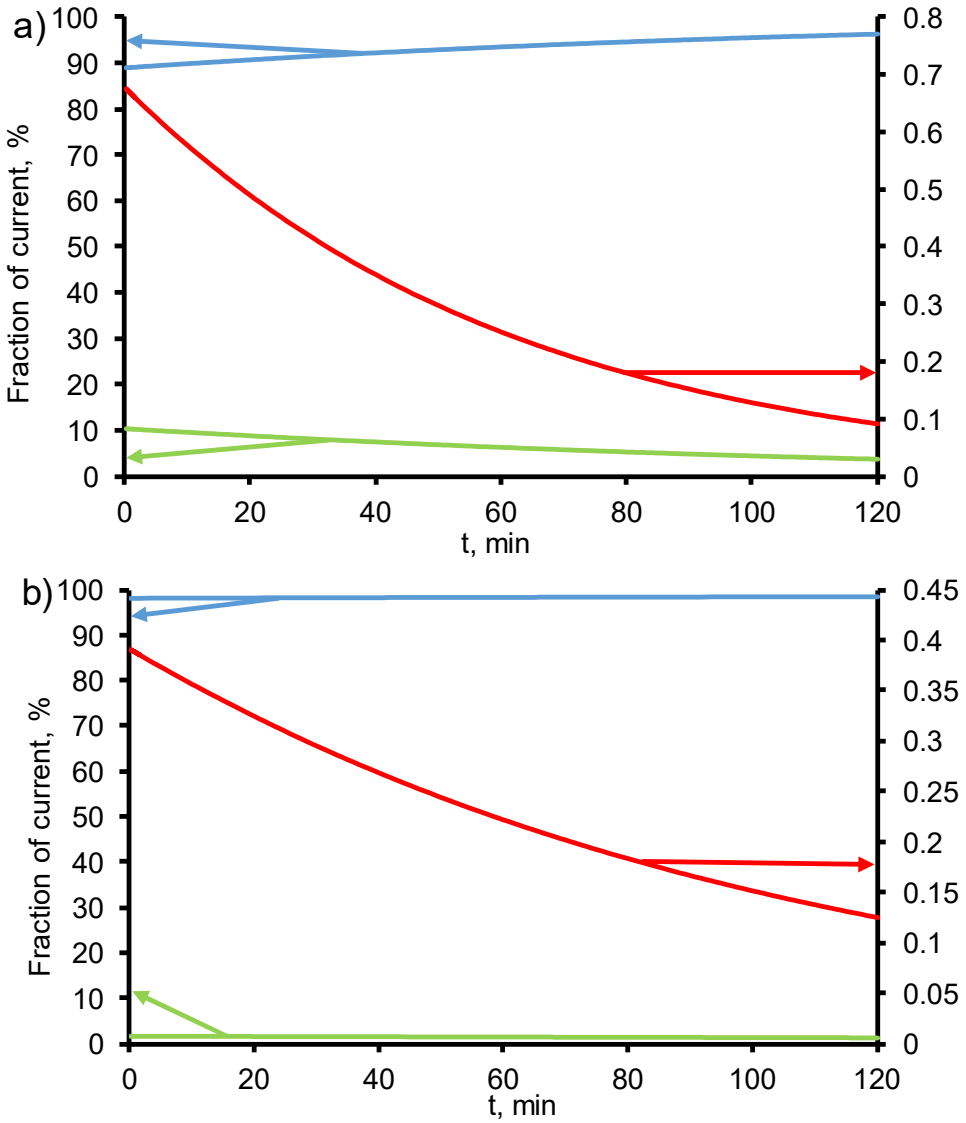

Figure 4 - Fractions of current spent on O_2 evolution (blue line), terephthalic acid (TA) oxidation by $^{\bullet}OH$ (red line) and mineralization of degradation by-products (green line) on BDD (a) and TiOx (b) electrodes at 5 mA cm^{-2}. The secondary y-axis refers to the fraction of current spent on TA oxidation.

4.4 Oxidation of PCT by direct electron transfer using a quencher of hydroxyl radicals

PCT was selected as a model compound since it can potentially react during electro-oxidation by both DET and $^{\bullet}OH$-mediated oxidation. Ethanol was used as a quencher of both $^{\bullet}OH$ and $SO_4^{\bullet-}$. TBA was used as a quencher of only $^{\bullet}OH$ as it reacts slowly with $SO_4^{\bullet-}$ [45–47]. None significant difference was obtained by using both quenchers (**Fig. SI-8**), which indicated the suitability of

not considering $SO_4^{\bullet-}$-mediated oxidation for this specific case. Only DET and $^{\bullet}OH$-mediated oxidation were considered for modeling. Diffusion coefficient of PCT was obtained from the literature, while the one of ethanol was considered as equal to the one of PCT. Reaction rate constants for mineralization of ethanol by $^{\bullet}OH$ and degradation of PCT with $^{\bullet}OH$ were obtained from the literature. The thickness of the diffusion layer was taken from values calibrated in section 4.3. Conditions for $^{\bullet}OH$ generation were kept as descrived in section 4.2. Thus, all conditions for $^{\bullet}OH$-based reactions were considered as established. Mineralization of PCT by-products was calibrated in the following experiments without quenchers. However, as mentioned in section 4.3 and detailed in section 4.6, mineralization of PCT by-products was not a parameter affecting degradation kinetic of the initial compound. Thus, experimental data obtained for PCT oxidation with ethanol as quencher (**Fig. 5A**) were used for calibration of the formal potential related to DET of PCT (**Eq. 16, SI**) at the surface of BDD and TiO_x electrodes.

Faster removal of PCT was obtained with BDD anode compared to TiO_x. It was necessary to consider a more favorable reactivity of PCT for DET at BDD anode (E°_{PCT} = 2.38 and 3.30 V *vs* Ag/AgCl for BDD and TiO_x, respectively) in order to fit with the experimental data. Such better electrokinetic behavior of BDD for DET indicate that it might also be an important parameter to take into consideration for explaining the faster mineralization rates obtained with BDD compared to TiO_x.

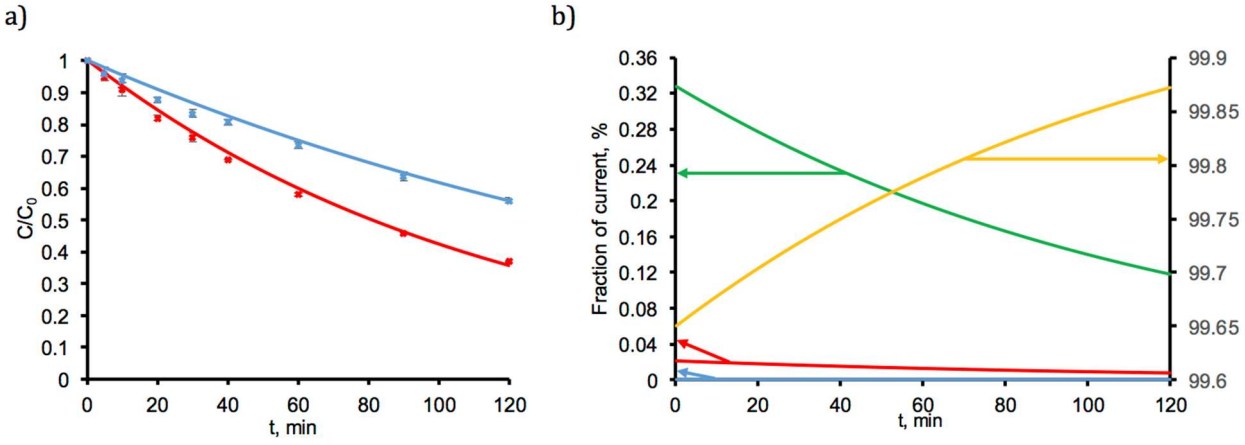

Figure 5 – (a) Experimental (dots) *vs* model (lines) data for paracetamol (PCT) degradation on BDD (red) and TiOx (blue) electrodes (at 5 mA cm^{-2}) in the presence of ethanol. Error bars (sometimes contained within dots) corresponds to triplicate experiments. (b) Fractions of current spent on O_2 evolution (blue line), PCT oxidation by •OH (red line), PCT oxidation by DET (green line), ethanol oxidation (yellow line) during PCT oxidation on BDD electrode in the presence of ethanol. The secondary y-axis refers to the fraction of current spent on ethanol oxidation.

Calculations showed that using a concentration of 100 mM of ethanol was suitable for quenching •OH. In such conditions with a high concentration of ethanol, the system was operated under current limitation ($j<j_{lim}$). Ethanol provided a huge pathway for the disappearance of •OH and the reaction layer thickness decreased to 5 nm (160 times less than without ethanol) with a maximum surface concentration of •OH around 0.2 µM (100 times lower than without ethanol) (**Fig. SI-9**). This presence of ethanol strongly decreased the possibility of PCT to react with •OH. At time t = 0 with the BDD anode, the calculated fraction of current spent for PCT degradation by •OH-mediated oxidation was only 0.02% while it was 0.33% for PCT degradation by DET (**Fig. 5B**). After 2 hours of treatment, it was calculated that only 6.1% of the degradation yield of PCT was ascribed to •OH (**Fig. SI-11**). A similar trend was obtained with TiO_x anode (**Fig. SI-10 and SI-11**). The fraction of PCT removed by •OH (11.0%) was slightly higher as it was calibrated that the reaction of PCT through DET is less favorable at the TiO_x anode.

Further calculations were performed in order to assess the relevance of using different concentration of ethanol in the case of the BDD electrode. Using a concentration of 10 mM would increase the fraction of current spent on •OH-mediated oxidation of PCT from 0.02 to 0.17% (at time t = 0). On the contrary, the fraction of current spent on PCT oxidation by DET would decrease from 0.33 to 0.25% (i.e., in the same ordre of magnitude than for •OH-mediated oxidation). Thus, decreasing the concentration of ethanol to 10 mM would not allow for reaching

455 sufficient quenching effect, even if it corresponds to a high ratio between ethanol and the target
456 pollutant (10/0.1 = 100).

457

458 **4.5 Oxidation of PCT without quencher**

459 A similar experiment was then performed without the addition of any •OH scavenger. Only DET
460 and •OH-mediated oxidation were considered for modeling. Diffusion coefficient and reaction
461 rate constants of PCT with •OH was obtained from the literature, while the one of ethanol was
462 considered as equal to the one of PCT. The thickness of the diffusion layer was taken from
463 values calibrated in section 4.3. Conditions for •OH generation were kept as descrived in section
464 4.2. Conditions for oxidation of PCT by DET were taken from the values calibrated in section
465 4.4. Thus, all model parameters were taken from previous experiments (or from literature) and
466 good agreement was observed between experimental and model values obtained for the
467 degradation kinetic of PCT (**Fig. 6A**). Besides, the global reaction rate of degradation by-
468 products was calibrated from experimental data of TOC removal. As mentioned in previous
469 sections and detailed in section 4.6, mineralization of by-products was not a phenomenon
470 affecting degradation kinetic of the initial compound. The diffusion coefficient of by-products
471 was taken as equal to PCT. The total amount of •OH consumed per molecule of by-product
472 mineralized was calculated according to the equation given in SI (**Eq. 8, SI**).

473 As observed previously, PCT can react through both DET and •OH-mediated oxidation.
474 However, calculations highlighted that PCT was almost exclusively degraded through •OH-
475 mediated oxidation in these conditions (i.e., absence of quenchers, mass transport limitation).
476 With BDD anode, at time t = 0, 0.68% of the current was spent on degradation of PCT by •OH
477 while it was only 0.0022% for DET (**Fig. 6B**). After 2 h of treatment, it was calculated that more
478 than 99.99% of PCT was removed by •OH-mediated oxidation (**Fig. SI-11**). Similar trend was
479 obtained with TiO_x anode (**Fig. SI-11 and SI-12**). In fact, PCT is able to react rapidly in the
480 reaction zone where •OH are accumulated and a very low amount of PCT reaches the electrode

surface (x = 0) for reacting through DET. This phenomenon was clearly emphasized in **Fig. 7** for BDD and **Fig. SI-13** for TiO_x. PCT molecules are able to reach the electrode surface for reaction through DET only when ethanol was added as quencher of •OH, while concentration of PCT was 0 at the electrode surface in absence of •OH quencher. All PCT molecules are able to react very fast with •OH in the reaction zone when the process is operated under mass transport limitation. These results emphasized that different degradation mechanisms and pathways might happen depending on operating conditions (presence of radical scavengers, mass transport *vs* current limitation).

As observed with TA, a more important difference was observed between TiO_x and BDD for mineralization rate, compared to degradation rate. For example, the mineralization yield of PCT after 2 h of treatment was 14 and 66% for TiO_x and BDD, respectively, while the degradation yield after 1 h was 44 and 67% for TiO_x and BDD, respectively. As explained above, it might be related to the better electrokinetic behavior of BDD for mineralization of by-products more refractory to •OH and/or by the evolution at the TiO_x electrode of a greater amount of •OH through waste reactions of **Eqs. 8-10**.

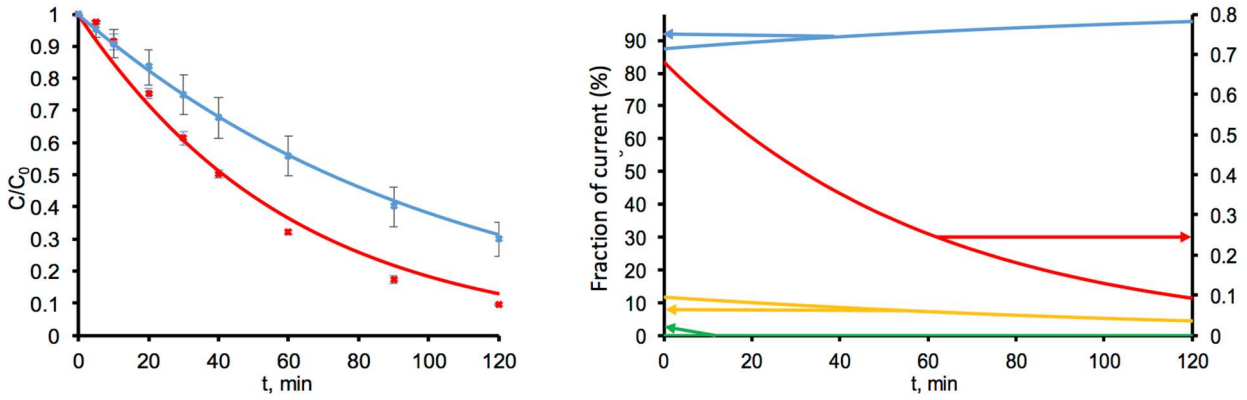

Figure 6 – (a) Experimental (dots) vs model (lines) data for paracetamol (PCT) degradation on BDD (red) and TiOx (blue) electrodes (at 5 mA cm^{-2}) in the absence of ethanol. Error bars (sometimes contained within dots) corresponds to triplicate experiments. (b) Fractions of current spent on O_2 evolution (blue line), PCT oxidation by •OH (red line), PCT oxidation by DET

(green line), mineralization of degradation by-products (yellow line) during PCT oxidation on BDD electrode in the absence of ethanol. The secondary y-axis refers to the fraction of current spent on PCT oxidation by •OH.

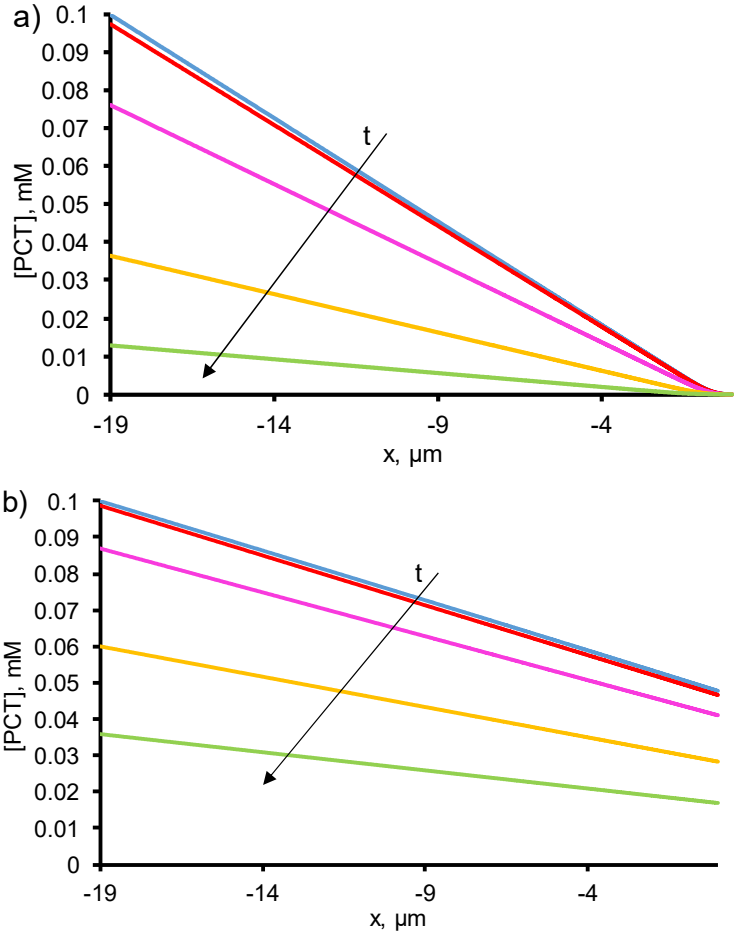

Figure 7 - Concentration profiles of PCT during the PCT oxidation on BDD electrode in the absence (a) and in the presence (b) of ethanol at t = 10 (blue), 100 (red), 1000 (pink), 3600 yellow), 7200 (green) s.

4.6 Sensitivity analysis: competition between the initial compound and by-products

As soon as the electro-oxidation starts, the solution contains the initial target molecule as well as the degradation by-products. Therefore, there is a potential competition between these different compounds for reaction with •OH. The objective of this section was to study whether this competition might have a significant effect on degradation kinetic of the target compound.

For this purpose, the influence of two characteristics of by-products was tested, including (i) the reaction rate constant with •OH (k_{BP}) and (ii) the diffusion coefficient of by-products, which might affect mass transport conditions. Interestingly, calculations showed that the variation of these values did not affect significantly PCT degradation kinetics (**Fig. 8A and 8B**). It was previously observed that a higher amount of current is actually spent on mineralization of by-products compared to initial degradation of PCT. However, under mass transport limitation, it still represents a low fraction of the total current provided (e.g. less than 4.2% after 2 h of treatment in the conditions of **Fig. 6**). Thus, competition effects are not significant since the reaction rate of •OH with by-products does not significantly modify the amount of •OH available for reaction with PCT.

In this study, mineralization of by-products was considered to occur only through •OH-mediated oxidation. Actually, DET could also participate. Therefore, the amount of hydroxyl radicals used for mineralization is overestimated with this model. Despite this overestimation, this study highlighted that the consumption of •OH by reaction with by-products does not affect the degradation kinetic of TA at BDD anode when operating AO under mass transport limitation.

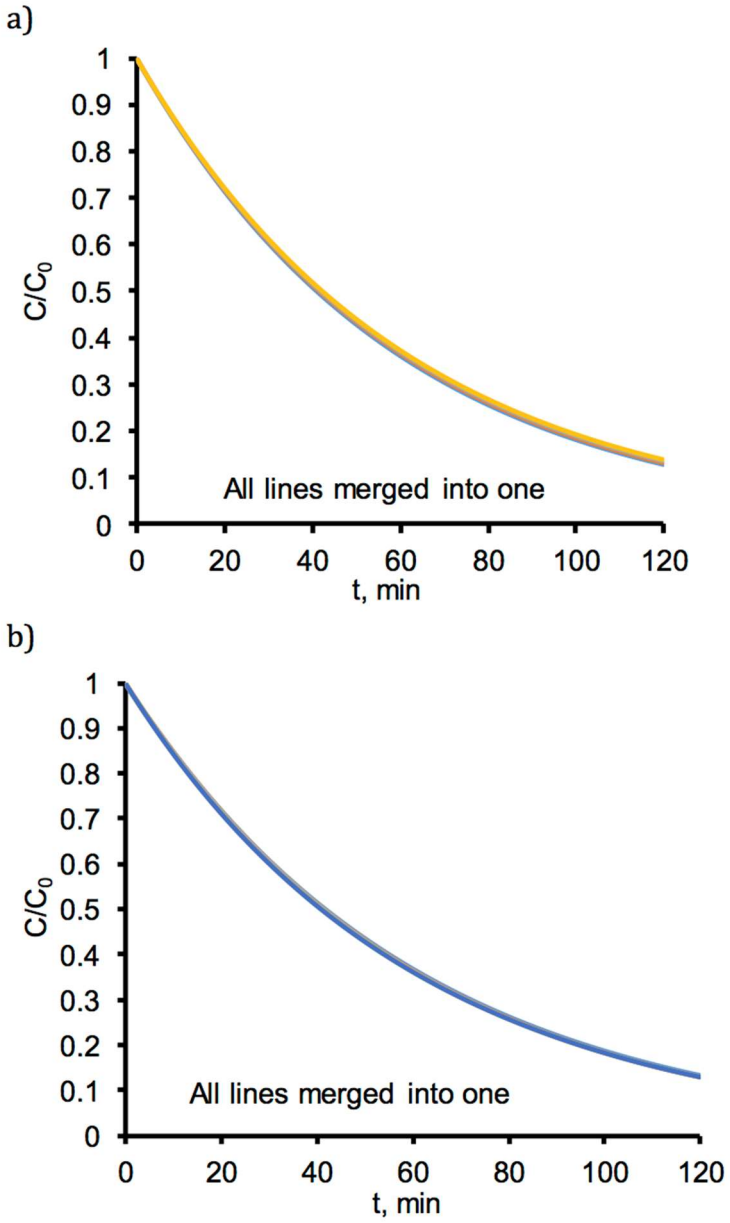

Figure 8 – (a) Calculated degradation kinetics of PCT on BDD electrode (in the absence of ethanol) at different values of reaction rate constant of by-products with •OH, $k_{BP} = 0.001 \cdot k_{PCT}, 0.01 \cdot k_{PCT}, 0.1 \cdot k_{PCT}, k_{PCT}$ $m^3 / (mol \cdot s)$. (b) Calculated degradation kinetics of PCT on BDD electrode (in the absence of ethanol) at different values of diffusion coefficient of by-products, $D_{BP} = 0.01 \cdot D_{PCT}, 0.1 \cdot D_{PCT}, D_{PCT}, 10 \cdot D_{PCT}, 100 \cdot D_{PCT}$ m^2 / s

4.7 Sensitivity analysis: influence of target compound reactivity with hydroxyl radicals

The next objective was to study the influence of target compound reactivity with •OH. The first case studied was that of a molecule strongly refractory to DET such as TA. All model parameters were taken from the sub-section 4.3 on TA degradation and the influence of the value of the reaction rate constant with •OH (k_{TA}) was tested (**Fig. 9A**).

There was not any significant effect of k_{TA} in the range for values above 10^6 m^3 mol^{-1} s^{-1}. In this range of values, •OH generated in the reaction zone were sufficient to oxidize all target compounds under mass transport control (i.e., the concentration of target compound at electrode surface, x = 0, was always 0). Therefore, the effectiveness of the process depends only on mass transport conditions. The degradation kinetic starts decreasing only from k_{TA} = 10^5 m^3 mol^{-1} s^{-1} and further strongly drops at 10^4 and 10^3 m^3 mol^{-1} s^{-1}. In this range of values, the degradation of the target compound is kinetically limited by the reaction with •OH. The amount of •OH in the reaction zone is not sufficient to oxidize all target compounds because the reaction kinetic is too slow. Increasing the current density (and therefore the amount of generated •OH) would counteract such phenomenon for increasing degradation kinetic. Thus, even under mass transport limitation according to **Eq. 3**, the current intensity would also play a role on the removal of the most recalcitrant compounds.

The second case studied was that of a molecule that can potentially react through both DET and •OH mediated oxidation such as PCT. All model parameters were taken from the sub-sections 4.4 and 4.5 on PCT degradation. The influence of the value of the reaction rate constant with •OH (k_{PCT}) was tested (**Fig. 9B**). As in the first case and for the same reason, there was not any significant effect of k_{PCT} in the range 10^6 – 10^8 m^3 mol^{-1} s^{-1}. Then, the degradation kinetics of the target compound decreased for lower values but a much lower decrease was observed compared to the first case. In fact, target compounds that do not fully react in the reaction zone with •OH can reach the electrode surface and react by DET. In such case, DET would participate to counteract the slow reaction with •OH. These calculations show that electrokinetic parameters

583 related to DET might play a key role on the removal of organic compounds that are the most
584 recalcitrant to reaction with •OH.

585 For example, oxalic acid is a well-known end by-products of degradation of organics by
586 AOPs/EAOPs. It is difficult to remove because of its slow reaction with •OH (k_{OA} = 1.4 x 10^3 m^3
587 mol^{-1} s^{-1}). With such a reaction rate constant, its reactivity through DET might make important
588 differences. It is the reason why DET is also an important phenomenon to take into consideration
589 for comparing the effectiveness of non-active electrodes for achieving complete mineralization
590 of organic pollutants.

591

592

593

594

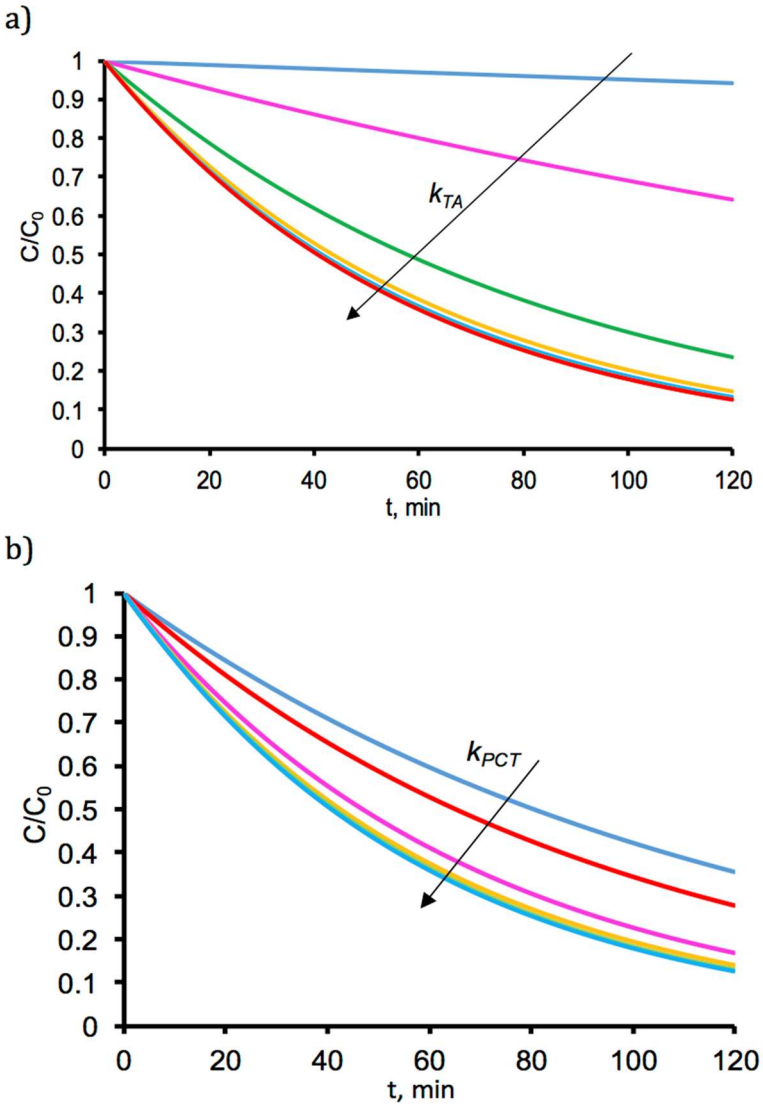

Figure 9 – (a) Degradation kinetics of terephthalic acid (TA) on BDD electrode at different values of reaction rate constant of TA with •OH, k_{TA} = 3.3 x 10^3 (blue), 3.3 x 10^4 (pink), 3.3 x 10^5 (green), 3.3 x 10^6 (yellow), 3.3 x 10^7 (red) m^3 mol^{-1} s^{-1}. (b) Degradation kinetics of paracetamol (PCT) on BDD electrode at different values of reaction rate constant of PCT with •OH, k_{PCT} = 10^3 (blue), 10^4 (red), 10^5 (pink), 10^6 (yellow), 10^7 (green) m^3 mol^{-1} s^{-1}.

4.8 Sensitivity analysis: influence of mass transport coefficient

Under mass transport limitation, mass transport conditions obviously influence strongly the degradation kinetic of the target compound. As observed in **Fig. 10**, the change of the mass transport coefficient by one order of magnitude has a huge effect on degradation kinetic. It is the

reason why a great attention is currently given to the development of porous electrodes that can be implemented under flow-through configuration. Using electrodes with pore size lower than the diffusion boundary layers allows for reducing adverse effects from diffusion phenomena. Thus, mass transport can be effectively improved by increasing the convective flux through the porous electrode.

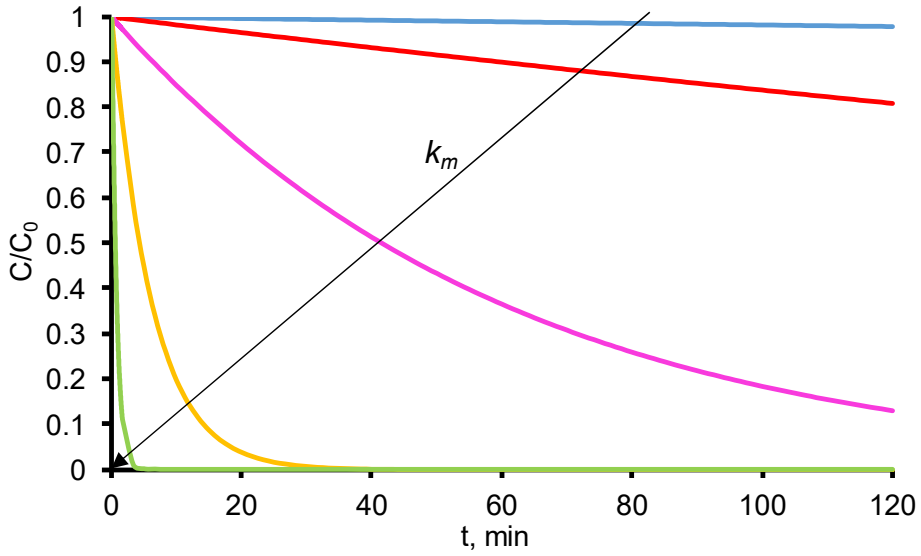

Figure 10 – Degradation kinetics of PCT on BDD electrode at different values of mass transport coefficient, k_m = 3.4 x 10^{-7} (blue), 3.4 x 10^{-6} (red), 3.4 x 10^{-5} (pink), 3.4 x 10^{-4} (yellow), 3.4 x 10^{-3} (green) m s^{-1}.

4.9 Sensitivity analysis: influence of the ratio S/V

As observed in **Table 1**, it is difficult to compare data obtained from the literature since they have been obtained in different operating conditions. When the anodic oxidation process is applied under mass transport limitation, one crucial parameter is for example the ratio between the geometric surface area of the electrode and the volume of the treated solution (S/V). Results presented in **Fig. 11A** presents the influence of this ratio on the degradation kinetic of PCT using BDD anode, as calculated from the model. The calculated value of k_{app} is strongly improved by simply increasing this ratio. **Fig. 11B** shows the linear correlation obtained between k_{app} and the

ratio S/V. The value of k_{app} (in min^{-1}) was directly proportional to the ratio S/V (in m^{-1}). This value of the S/V ratio should be further taken into consideration for the comparison of results obtained in different studies.

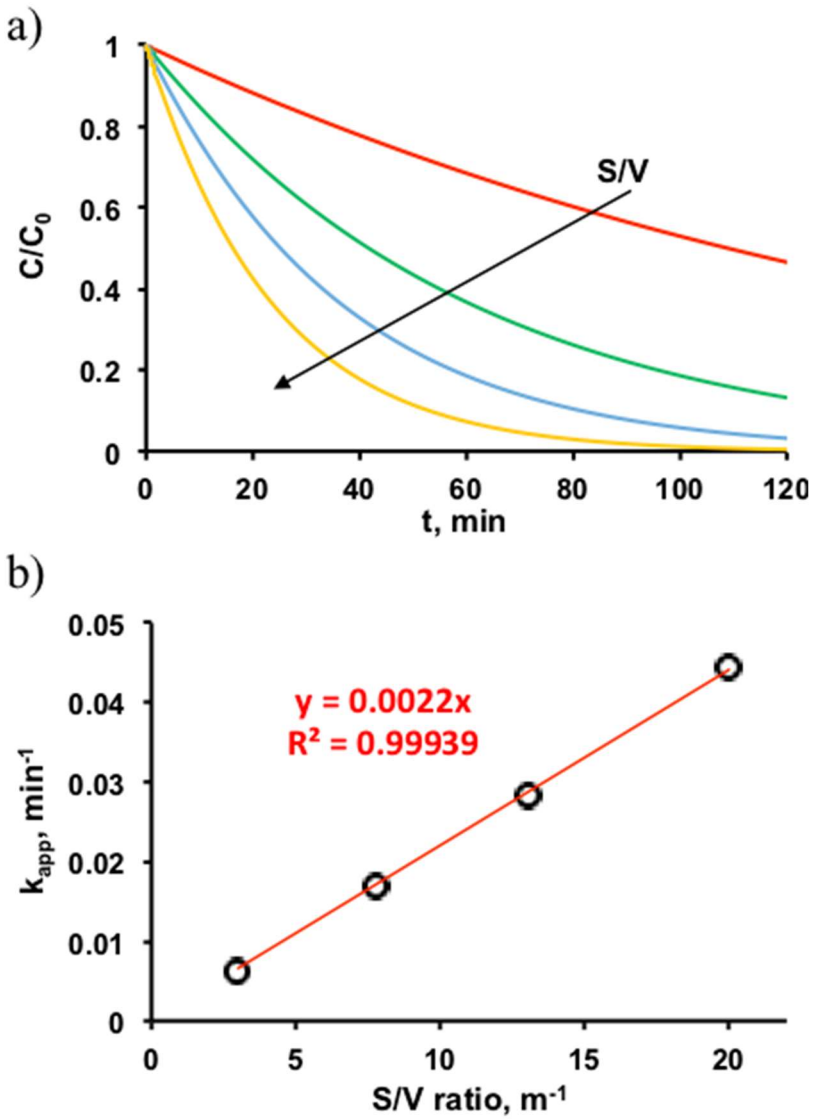

Figure 11 – Influence of the ratio between electrode surface (S) and solution volume (V) on the degradation kinetic of PCT using BDD anode, as calculated from the model. (a) Degradation kinetics obtained for S/V = 3 (red), 7.8 (green), 13 (blue) and 20 (yellow). (b) Pseudo-first order rate constant (k_{app}) according to the S/V ratio.

5. Conclusions

Combination of both experimental and modeling approaches allowed for better understanding the reactivity of non-active electrodes such as BDD and TiO_x. A mathematical model taking into account both •OH-mediated oxidation and DET was developed and calibrated using experimental data. The fraction of current spent in the different possible reactions was calculated and allowed for discussion of the predominant reaction mechanism accoding to the experimental configuration.

Results showed that organic compounds are fully oxidized by •OH when (i) the process is operated under mass transport control and (ii) the reaction rate constant with •OH is sufficiently high. Moreover, none significant competition between the mother molecule and degradation by-products was observed under mass transport limitation. The role of DET become potentially crucial for the removal of organic compounds with low reaction rates with •OH (below $k < 10^5$ m^3 mol^{-1} s^{-1}) and/or in presence of large amounts of •OH scavengers. Thus, electrokinetic parameters related to DET might also play a key role for achieving complete mineralization of organic compounds and for application of the process under current limitation.

The use of radical quenchers is currently widely used in the litterature for identification of reactive species during oxidation processes. The results obtained in this study showed that a concentration of 100 mM of ethanol was required to ensure that •OH-mediated oxidation was not significant at 5 mA cm^{-2} and for a concentration of target compound of 0.1 mM.

Finally, degradation kinetics obtained with TiO_x electrodes were close to that obtained with BDD, even for a •OH probe molecule such as TA. However, the mineralization power of TiO_x was lower; further investigations are required to clearly identify the underlying reasons. Particularly, further investigations are required to better understand the different mechanisms related to OER and formation of •OH at the surface of these anodes.

Acknowledgments

Jing Ma thanks China Scholarship Council for supporting her PhD work in Université Gustave Eiffel. Authors acknowledge Saint-Gobain Research Provence for providing TiO_x electrodes. This research was partially funded by the Ministry of Education and Science of the Russian Federation (project No. FZEN-2020-0022).

References

[1] I. Sirés, E. Brillas, M.A. Oturan, M.A. Rodrigo, M. Panizza, Electrochemical advanced oxidation processes: today and tomorrow. A review, Environmental Science and Pollution Research. 21 (2014) 8336–8367. https://doi.org/10.1007/s11356-014-2783-1.

[2] J. Radjenovic, D.L. Sedlak, Challenges and Opportunities for Electrochemical Processes as Next-Generation Technologies for the Treatment of Contaminated Water, Environ. Sci. Technol. 49 (2015) 11292–11302. https://doi.org/10.1021/acs.est.5b02414.

[3] B.P. Chaplin, Critical review of electrochemical advanced oxidation processes for water treatment applications, Environmental Sciences: Processes and Impacts. 16 (2014) 1182–1203.

[4] C.A. Martínez-Huitle, M.A. Rodrigo, I. Sirés, O. Scialdone, Single and Coupled Electrochemical Processes and Reactors for the Abatement of Organic Water Pollutants: A Critical Review, Chem. Rev. 115 (2015) 13362–13407. https://doi.org/10.1021/acs.chemrev.5b00361.

[5] S.O. Ganiyu, C.A. Martínez-Huitle, M.A. Rodrigo, Renewable energies driven electrochemical wastewater/soil decontamination technologies: A critical review of fundamental concepts and applications, Applied Catalysis B: Environmental. 270 (2020) 118857. https://doi.org/10.1016/j.apcatb.2020.118857.

[6] C. Comninellis, Electrocatalysis in the electrochemical conversion/combustion of organic pollutants for waste-water treatment, Electrochim. Acta. 39 (1994) 1857–1862. https://doi.org/10.1016/0013-4686(94)85175-1.

[7] M. Panizza, G. Cerisola, Direct and mediated anodic oxidation of organic pollutants, Chem. Rev. 109 (2009) 6541–6569. https://doi.org/10.1021/cr9001319.

[8] A.V. Karim, P.V. Nidheesh, M.A. Oturan, Boron-doped diamond electrodes for the mineralization of organic pollutants in the real wastewater, Current Opinion in Electrochemistry. 30 (2021) 100855. https://doi.org/10.1016/j.coelec.2021.100855.

[9] M.A. Oturan, Outstanding performances of the BDD film anode in electro-Fenton process: Applications and comparative performance, Current Opinion in Solid State and Materials Science. 25 (2021) 100925. https://doi.org/10.1016/j.cossms.2021.100925.

[10] E. Brillas, C.A. Martínez-Huitle, Decontamination of wastewaters containing synthetic organic dyes by electrochemical methods. An updated review, Applied Catalysis B: Environmental. 166–167 (2015) 603–643. https://doi.org/10.1016/j.apcatb.2014.11.016.

[11] N. Oturan, E. Brillas, M.A. Oturan, Unprecedented total mineralization of atrazine and cyanuric acid by anodic oxidation and electro-Fenton with a boron-doped diamond anode, Environmental Chemistry Letters. 10 (2012) 165–170. https://doi.org/10.1007/s10311-011-0337-z.

[12] N. Oturan, E.D. van Hullebusch, H. Zhang, L. Mazeas, H. Budzinski, K. Le Menach, M.A. Oturan, Occurrence and Removal of Organic Micropollutants in Landfill Leachates Treated by Electrochemical Advanced Oxidation Processes, Environmental Science & Technology. 49 (2015) 12187–12196. https://doi.org/10.1021/acs.est.5b02809.

[13] C. Trellu, N. Oturan, Y. Pechaud, E.D. van Hullebusch, G. Esposito, M.A. Oturan, Anodic oxidation of surfactants and organic compounds entrapped in micelles – Selective degradation mechanisms and soil washing solution reuse, Water Research. 118 (2017) 1–11. https://doi.org/10.1016/j.watres.2017.04.013.

[14] C. Trellu, Y. Péchaud, N. Oturan, E. Mousset, D. Huguenot, E.D. van Hullebusch, G. Esposito, M.A. Oturan, Comparative study on the removal of humic acids from drinking water by anodic oxidation and electro-Fenton processes: Mineralization efficiency and modelling, Applied Catalysis B: Environmental. 194 (2016) 32–41. https://doi.org/10.1016/j.apcatb.2016.04.039.

[15] Á. Anglada, A.M. Urtiaga, I. Ortiz, Laboratory and pilot plant scale study on the electrochemical oxidation of landfill leachate, Journal of Hazardous Materials. 181 (2010) 729–

735. https://doi.org/10.1016/j.jhazmat.2010.05.073.

[16] K. Groenen-Serrano, E. Weiss-Hortala, A. Savall, P. Spiteri, Role of Hydroxyl Radicals During the Competitive Electrooxidation of Organic Compounds on a Boron-Doped Diamond Anode, Electrocatalysis. 4 (2013) 346–352. https://doi.org/10.1007/s12678-013-0150-5.

[17] M. Panizza, P.A. Michaud, G. Cerisola, Ch. Comninellis, Anodic oxidation of 2-naphthol at boron-doped diamond electrodes, Journal of Electroanalytical Chemistry. 507 (2001) 206–214. https://doi.org/10.1016/S0022-0728(01)00398-9.

[18] Q. Zhuo, S. Deng, B. Yang, J. Huang, G. Yu, Efficient Electrochemical Oxidation of Perfluorooctanoate Using a Ti/SnO2-Sb-Bi Anode, Environ. Sci. Technol. 45 (2011) 2973–2979. https://doi.org/10.1021/es1024542.

[19] S. Cotillas, D. Clematis, P. Cañizares, M.P. Carpanese, M.A. Rodrigo, M. Panizza, Degradation of dye Procion Red MX-5B by electrolytic and electro-irradiated technologies using diamond electrodes, Chemosphere. 199 (2018) 445–452. https://doi.org/10.1016/j.chemosphere.2018.02.001.

[20] J. Radjenovic, N. Duinslaeger, S.S. Avval, B.P. Chaplin, Facing the Challenge of Poly- and Perfluoroalkyl Substances in Water: Is Electrochemical Oxidation the Answer?, Environ. Sci. Technol. 54 (2020) 14815–14829. https://doi.org/10.1021/acs.est.0c06212.

[21] P.V. Nidheesh, G. Divyapriya, N. Oturan, C. Trellu, M.A. Oturan, Environmental Applications of Boron-Doped Diamond Electrodes: 1. Applications in Water and Wastewater Treatment, ChemElectroChem. 6 (2019) 2124–2142. https://doi.org/10.1002/celc.201801876.

[22] L. Guo, Y. Jing, B.P. Chaplin, Development and characterization of ultrafiltration TiO2 Magnéli phase reactive electrochemical membranes, Environmental Science & Technology. 50 (2016) 1428–1436.

[23] A.M. Zaky, B.P. Chaplin, Porous Substoichiometric TiO 2 Anodes as Reactive Electrochemical Membranes for Water Treatment, Environmental Science & Technology. 47 (2013) 6554–6563. https://doi.org/10.1021/es401287e.

[24] C. Trellu, C. Coetsier, J.-C. Rouch, R. Esmilaire, M. Rivallin, M. Cretin, C. Causserand, Mineralization of organic pollutants by anodic oxidation using reactive electrochemical membrane synthesized from carbothermal reduction of TiO2, Water Research. 131 (2018) 310–319. https://doi.org/10.1016/j.watres.2017.12.070.

[25] C. Trellu, M. Rivallin, S. Cerneaux, C. Coetsier, C. Causserand, M.A. Oturan, M. Cretin, Integration of sub-stoichiometric titanium oxide reactive electrochemical membrane as anode in the electro-Fenton process, Chemical Engineering Journal. 400 (2020) 125936. https://doi.org/10.1016/j.cej.2020.125936.

[26] S.O. Ganiyu, N. Oturan, S. Raffy, M. Cretin, R. Esmilaire, E. van Hullebusch, G. Esposito, M.A. Oturan, Sub-stoichiometric titanium oxide (Ti4O7) as a suitable ceramic anode for electrooxidation of organic pollutants: A case study of kinetics, mineralization and toxicity assessment of amoxicillin, Water Res. 106 (2016) 171–182. https://doi.org/10.1016/j.watres.2016.09.056.

[27] T.X.H. Le, H. Haflich, A.D. Shah, B.P. Chaplin, Energy-Efficient Electrochemical Oxidation of Perfluoroalkyl Substances Using a Ti4O7 Reactive Electrochemical Membrane Anode, Environ. Sci. Technol. Lett. 6 (2019) 504–510. https://doi.org/10.1021/acs.estlett.9b00397.

[28] N. Oturan, S.O. Ganiyu, S. Raffy, M.A. Oturan, Sub-stoichiometric titanium oxide as a new anode material for electro-Fenton process: Application to electrocatalytic destruction of antibiotic amoxicillin, Applied Catalysis B: Environmental. 217 (2017) 214–223. https://doi.org/10.1016/j.apcatb.2017.05.062.

[29] A. Kapałka, G. Fóti, C. Comninellis, The importance of electrode material in environmental electrochemistry: Formation and reactivity of free hydroxyl radicals on boron-doped diamond electrodes, Electrochimica Acta. 54 (2009) 2018–2023. https://doi.org/10.1016/j.electacta.2008.06.045.

[30] A. Kapałka, G. Fóti, C. Comninellis, Kinetic modelling of the electrochemical mineralization of organic pollutants for wastewater treatment, J Appl Electrochem. 38 (2008) 7–16. https://doi.org/10.1007/s10800-007-9365-6.

[31] C. Trellu, B.P. Chaplin, C. Coetsier, R. Esmilaire, S. Cerneaux, C. Causserand, M. Cretin, Electro-oxidation of organic pollutants by reactive electrochemical membranes, Chemosphere. 208 (2018) 159–175. https://doi.org/10.1016/j.chemosphere.2018.05.026.

[32] O. Simond, V. Schaller, Ch. Comninellis, Theoretical model for the anodic oxidation of organics on metal oxide electrodes, Electrochimica Acta. 42 (1997) 2009–2012. https://doi.org/10.1016/S0013-4686(97)85475-8.

[33] O. Scialdone, A. Galia, C. Guarisco, S. Randazzo, G. Filardo, Electrochemical incineration of oxalic acid at boron doped diamond anodes: Role of operative parameters, Electrochimica Acta. 53 (2008) 2095–2108. https://doi.org/10.1016/j.electacta.2007.09.007.

[34] O. Scialdone, Electrochemical oxidation of organic pollutants in water at metal oxide electrodes: A simple theoretical model including direct and indirect oxidation processes at the anodic surface, Electrochimica Acta. 54 (2009) 6140–6147. https://doi.org/10.1016/j.electacta.2009.05.066.

[35] Y. Lan, C. Coetsier, C. Causserand, K. Groenen Serrano, An experimental and modelling study of the electrochemical oxidation of pharmaceuticals using a boron-doped diamond anode, Chemical Engineering Journal. 333 (2018) 486–494. https://doi.org/10.1016/j.cej.2017.09.164.

[36] P. Cañizares, J. García-Gómez, J. Lobato, M.A. Rodrigo, Modeling of Wastewater Electro-oxidation Processes Part I. General Description and Application to Inactive Electrodes, Ind. Eng. Chem. Res. 43 (2004) 1915–1922. https://doi.org/10.1021/ie0341294.

[37] M. Mascia, A. Vacca, S. Palmas, A.M. Polcaro, Kinetics of the electrochemical oxidation of organic compounds at BDD anodes: modelling of surface reactions, J Appl Electrochem. 37 (2007) 71–76. https://doi.org/10.1007/s10800-006-9217-9.

[38] O. Scialdone, S. Randazzo, A. Galia, G. Silvestri, Electrochemical oxidation of organics in water: Role of operative parameters in the absence and in the presence of NaCl, Water Research. 43 (2009) 2260–2272. https://doi.org/10.1016/j.watres.2009.02.014.

[39] M. Mascia, A. Vacca, A.M. Polcaro, S. Palmas, J.R. Ruiz, A. Da Pozzo, Electrochemical treatment of phenolic waters in presence of chloride with boron-doped diamond (BDD) anodes: Experimental study and mathematical model, Journal of Hazardous Materials. 174 (2010) 314–322. https://doi.org/10.1016/j.jhazmat.2009.09.053.

[40] E. Mousset, Y. Pechaud, N. Oturan, M.A. Oturan, Charge transfer/mass transport competition in advanced hybrid electrocatalytic wastewater treatment: Development of a new current efficiency relation, Applied Catalysis B: Environmental. 240 (2019) 102–111. https://doi.org/10.1016/j.apcatb.2018.08.055.

[41] S.N. Misal, M.-H. Lin, S. Mehraeen, B.P. Chaplin, Modeling electrochemical oxidation and reduction of sulfamethoxazole using electrocatalytic reactive electrochemical membranes, Journal of Hazardous Materials. 384 (2020) 121420. https://doi.org/10.1016/j.jhazmat.2019.121420.

[42] E. Skolotneva, C. Trellu, M. Cretin, S. Mareev, A 2D Convection-Diffusion Model of Anodic Oxidation of Organic Compounds Mediated by Hydroxyl Radicals Using Porous Reactive Electrochemical Membrane, Membranes. 10 (2020) 102. https://doi.org/10.3390/membranes10050102.

[43] Y. Jing, B.P. Chaplin, Mechanistic Study of the Validity of Using Hydroxyl Radical Probes To Characterize Electrochemical Advanced Oxidation Processes, Environ. Sci. Technol. 51 (2017) 2355–2365. https://doi.org/10.1021/acs.est.6b05513.

[44] J. Xie, J. Ma, S. Zhao, T.D. Waite, Flow anodic oxidation: Towards high-efficiency removal of aqueous contaminants by adsorbed hydroxyl radicals at 1.5 V vs SHE, Water Research. 200 (2021) 117259. https://doi.org/10.1016/j.watres.2021.117259.

[45] J. Cai, M. Zhou, Y. Pan, X. Du, X. Lu, Extremely efficient electrochemical

degradation of organic pollutants with co-generation of hydroxyl and sulfate radicals on Blue-TiO2 nanotubes anode, Applied Catalysis B: Environmental. 257 (2019) 117902. https://doi.org/10.1016/j.apcatb.2019.117902.

[46] L. Zhou, C. Ferronato, J.-M. Chovelon, M. Sleiman, C. Richard, Investigations of diatrizoate degradation by photo-activated persulfate, Chemical Engineering Journal. 311 (2017) 28–36. https://doi.org/10.1016/j.cej.2016.11.066.

[47] G.P. Anipsitakis, D.D. Dionysiou, Radical Generation by the Interaction of Transition Metals with Common Oxidants, Environ. Sci. Technol. 38 (2004) 3705–3712. https://doi.org/10.1021/es035121o.

[48] P. Cañizares, J. García-Gómez, I. Fernández de Marcos, M.A. Rodrigo, J. Lobato, Measurement of Mass-Transfer Coefficients by an Electrochemical Technique, J. Chem. Educ. 83 (2006) 1204. https://doi.org/10.1021/ed083p1204.

[49] P.H.M. Janssen, P.S.C. Heuberger, Calibration of process-oriented models, Ecological Modelling. 83 (1995) 55–66. https://doi.org/10.1016/0304-3800(95)00084-9.

[50] P.-A. Michaud, M. Panizza, L. Ouattara, T. Diaco, G. Foti, C. Comninellis, Electrochemical oxidation of water on synthetic boron-doped diamond thin film anodes, Journal of Applied Electrochemistry. 33 (2003) 151–154. https://doi.org/10.1023/A:1024084924058.

[51] A.J. Bard, L.R. Faulkner, Electrochemical Methods: Fundamentals and Applications, Second, John Wiley and Sons, 2001.

[52] A. Kapałka, G. Fóti, C. Comninellis, Determination of the Tafel slope for oxygen evolution on boron-doped diamond electrodes, Electrochemistry Communications. 10 (2008) 607–610. https://doi.org/10.1016/j.elecom.2008.02.003.

[53] E. Brillas, I. Sirés, M.A. Oturan, Electro-Fenton process and related electrochemical technologies based on Fenton's reaction chemistry, Chemical Reviews. 109 (2009) 6570–6631. https://doi.org/10.1021/cr900136g.

[54] G. Buxton, C. Greenstock, W. Helman, A. Ross, Critical-Review of Rate Constants for Reactions of Hydrated Electrons, Hydrogen-Atoms and Hydroxyl Radicals (.oh/.o-) in Aqueous-Solution, J. Phys. Chem. Ref. Data. 17 (1988) 513–886.

[55] X. Fang, G. Mark, C. von Sonntag, OH radical formation by ultrasound in aqueous solutions Part I: the chemistry underlying the terephthalate dosimeter, Ultrasonics Sonochemistry. 3 (1996) 57–63. https://doi.org/10.1016/1350-4177(95)00032-1.

[56] N. Oturan, J. Bo, C. Trellu, M.A. Oturan, Comparative Performance of Ten Electrodes in Electro-Fenton Process for Removal of Organic Pollutants from Water, ChemElectroChem. 8 (2021) 3294–3303.

[57] A. El-Ghenymy, F. Centellas, J.A. Garrido, R.M. Rodríguez, I. Sirés, P.L. Cabot, E. Brillas, Decolorization and mineralization of Orange G azo dye solutions by anodic oxidation with a boron-doped diamond anode in divided and undivided tank reactors, Electrochimica Acta. 130 (2014) 568–576. https://doi.org/10.1016/j.electacta.2014.03.066.

[58] E. Brillas, I. Sirés, C. Arias, P.L. Cabot, F. Centellas, R.M. Rodríguez, J.A. Garrido, Mineralization of paracetamol in aqueous medium by anodic oxidation with a boron-doped diamond electrode, Chemosphere. 58 (2005) 399–406. https://doi.org/10.1016/j.chemosphere.2004.09.028.